Macromolecules
ARTICLE

Macromolecules **2009**, *42*, 4491–4499 **4491**
DOI: 10.1021/ma900623p

Energy Level and Molecular Structure Engineering of Conjugated Donor−Acceptor Copolymers for Photovoltaic Applications

Yaowen Li, Lili Xue, Hui Li, Zaifang Li, Bin Xu, Shanpeng Wen, and Wenjing Tian*

State Key Laboratory of Supramolecular Structure and Materials, Jilin University, Changchun 130012, P. R. China

Received March 23, 2009; Revised Manuscript Received April 28, 2009

ABSTRACT: A series of novel soluble conjugated copolymers consisting of coplanar donor (bithiophene-vinyl)−acceptor (2-pyran-4-ylidenemalononitrile) (TVM)-based unit coupled to different electron-donating ability moieties were synthesized by Suzuki coupling polymerization. The structures of the copolymers were characterized, and their physical properties were investigated. High molecular weight (M_n up to 43.8 kg/mol) and thermostable copolymers were obtained. The combination of TVM unit building block with gradually increased electron-donating ability moieties results in enhanced $\pi-\pi$ stacking in solid state and intramolecular charge transfer (ICT) transition bands, which lead to an extension of their absorption spectral range. Cyclic voltammetry measurement displayed that the highest occupied molecular orbital (HOMO) and lowest unoccupied molecular orbital (LUMO) energy levels of the copolymers can be fine-tuned. The resulting copolymers possessed relatively low HOMO energy levels promising good air stability and high open-circuit voltage (V_{oc}) for photovoltaic application. Bulk heterojunction photovoltaic devices were fabricated by using the copolymers as donors and (6,6)-phenyl C_{61}-butyric acid methyl ester (PCBM) as acceptor. It was found that the V_{oc} reached 0.90 V, and the power conversion efficiencies (PCE) of the devices were measured between 0.04% and 0.99% under simulated AM 1.5 solar irradiation of 100 mW/cm^2. The significant improvement of PCE indicates a novel concept for developing TVM-based donor−acceptor (D−A) conjugated copolymers with high photovoltaic performance by adjusting electron-donating ability and coplanarity.

Introduction

In recent years, considerable efforts have been directed toward the development of new polymer photovoltaic cells (PVCs). They are becoming more and more attractive because they represent a low cost and flexible devices, tunable electronic properties, and ease of processing.[1−4] One of the promising strategies for devising efficient PVCs involves the use of interpenetrating networks bulk heterojunctions (BHJ) based on a blend of electron-donating conjugated polymers and soluble fullerene acceptors as the active layer.[5] For instance, bulk heterojunction PVCs made from a blend of regioregular poly(3-hexylthiophene) (P3HT) and PCBM as the acceptor have recently been shown the power conversion efficiencies (PCE) up to 4−5%.[6] However, P3HT only harvests photons with wavelengths below 650 nm, while the energy of the majority of the solar photons is much lower (around 700 nm).[7] In order to further improve the properties of PVCs, people paid more attention to the D−A conjugated polymers whose optical and electronic properties could be tunable through the intramolecular charge transfer (ICT) from donor to acceptor. So, design and synthesis of D−A conjugated copolymers which can efficiently harvest the majority energy of the solar spectrum are effective ways to obtain low-band-gap polymers.[8] However, several reported D−A copolymers based on fused thiophene ring systems showed PCE much lower than the wide-band-gap counterparts[9] because of the mismatch of the energy level between electron-donating polymer and electron acceptor (e.g., PCBM), small light absorption coefficient, and large-scale blend phase separation between donor and acceptor. Most recently, several D−A copolymer systems have achieved better efficiency by tuning the energy level of the polymers through modifying the monomer structures based on the known thienopyrazine or benzothiadiazole systems.[10] However, the relatively low V_{oc} (around 0.6 V) still limits the PCE of the devices.

On all accounts, the D−A copolymers with low band gaps are needed for harvesting solar photons in a broader spectrum. To fulfill this requirement, well-chosen donor and acceptor group are particularly desirable for low-band-gap polymers due to a significant enhancement of the ICT intensity and conjugated length, which lead to a better extended absorption and higher absorption coefficient. In addition, the D−A copolymers should possess the following two features in order to achieve high efficiency of PVCs. One is sufficient driving force for electron transfer from the electron donor to the acceptor and suitable HOMO energy level of electron donor. It means that the LUMO energy level of the electron donor must be higher enough than that of the electron acceptor (at least 0.3 eV) in order to have sufficient driving force for electron transfer from donor to acceptor, and the HOMO energy level of electron donor must be low enough in order to get relative high V_{oc} which is determined by the difference between the HOMO energy level of donor and LUMO energy level of acceptor.[13] The other is to have good miscibility with the electron acceptor (e.g., PCBM) to form an interpenetrating network. In order to efficiently dissociate the excitons that occurred at the interface between the electron-donating component and the electron-accepting one, the control of the BHJ morphology is of crucial importance. Ideally, the phase-separation length scale should match the exciton diffusion length of conjugated polymer, which is ~10 nm.[11] Introduction of more rigid planar moieties to form coplanar structure copolymer has been proven to be an effective

*Corresponding author: e-mail wjtian@ jlu.edu.cn; Tel +86431 85155359; Fax +86431 85193421.

Published on Web 05/12/2009

approach to minimize the phase separation because the coplanar structure is benefit to enhance the $\pi-\pi$ stacking of the copolymers in solid state.[12] Consequently, to further increase the photovoltaic performances for practical application, it is important to design and synthesize polymers with the possibility to tune their energy levels and the coplanar molecular structure.

Herein, we synthesized three novel π-conjugated copolymers consisting of TVM-based donor unit coupled to different electron-donating moieties: poly{(9,9-dihexyl-9*H*-fluorene-2,7-ylene)-*alt*-2-(2,6-bis((*E*)-2-(5-bromo-3,4-dihexylthiophen-2-yl)vinyl)-4*H*-pyran-4-ylidene)malononitrile} (PFTMT), poly{(10-hexyl-10*H*-phenothiazine-3,7-ylene)-*alt*-2-(2,6-bis((*E*)-2-(5-bromo-3,4-dihexylthiophen-2-yl)vinyl)-4*H*-pyran-4-ylidene)malononitrile} (PPTMT), and poly{(2,2′-bithiophene-5,5′-ylene)-*alt*-2-(2,6-bis((*E*)-2-(5-bromo-3,4-dihexylthiophen-2-yl)vinyl)-4*H*-pyran-4-ylidene)malononitrile} PDTTMT. 2-Pyran-4-ylidenemalononitrile is a strong electron-accepting group, which can increase electron affinity and reduce the band gap of the conjugated system.[14] The symmetrical combination of 2-pyran-4-ylidenemalononitrile with alkylated thiophenevinyl assured the better conjugated length and coplanarity, which could further reduce the band gap of the conjugated system. We reasoned that incorporation of functional electron-donating moieties into the TVM-based copolymers with different electron-donating ability will bring different degrees of ICT to the conjugated system and thus provide a means to tune the energy levels. Indeed, we found that the energy level and absorption spectra of copolymers can be fine-tuned by changing the moieties of different electron-donating ability. Both the HOMO energy level (−5.25 to −5.63 eV) and LUMO energy level (around −3.56 eV) of the copolymers were in the range of ideal energy level.[2b] The photovoltaic performances of copolymers demonstrated that appropriate energy level and molecular structure engineering resulted in the improvement of the PCE to 0.99% (in the case of PDTTMT), which was more than 23 times higher than that of PFTMT.

Experimental Section

Materials. 9,9-Di-*n*-hexylfluorene (**6**), 10-hexylphenothiazine (**9**), 2-(2,6-dimethylpyran-4-ylidene)malononitrile, and 2,2′-bithiophene (**12**) were synthesized according to the literature procedures.[15−18] All reagents and chemicals were purchased from commercial sources (Aldrich, Across, and Fluka) and used without further purification unless stated otherwise. All solvents were distilled over appropriate drying agent(s) prior to use and were purged with nitrogen.

General Procedures of Polymerization. Suzuki cross-coupling reaction was used to synthesize the polymers shown in Scheme 2. 2,7-Bis(4,4,5,5-tetramathyl-1,3,2-dioxaborolan-2-yl)-9,9-dihexylfluorene, 10-hexyl-3,7-bis(4,4,5,5-tetramethyl-1,3,2-dioxaborolan-2-yl)-10*H*-phenothiazine, 5,5′-bis(4,4,5,5-tetramethyl-1,3,2-dioxaborolan-2-yl)-2,2′-bithiophene, dibromo monomer (TPMT), and $(PPh_3)_4Pd(0)$ (2 mol % with respect to the monomer) were dissolved in a mixture of toluene (15 mL) and aqueous 2 M K_2CO_3 (3/2 volume ratio). The solution was stirred under an Ar atmosphere and refluxed with vigorous stirring for 48 h. The resulting solution was then poured into methanol and followed by washing with water. The precipitated solid was extracted with methanol and acetone for 24 h in a Soxhlet apparatus to remove the oligomers and catalyst residues, respectively. The soluble fraction is then collected via extraction with $CHCl_3$ for 24 h. The chloroform solution is then concentrated to afford the copolymers.

Poly{(9,9-dihexyl-9*H*-fluorene-2,7-ylene)-*alt*-2-(2,6-bis((*E*)-2-(5-bromo-3,4-dihexylthiophen-2-yl)vinyl)-4*H*-pyran-4-ylidene)malononitrile} (PFTMT). The resulting polymer PFTMT was obtained as a dark green shining powder with a yield of 80%. ^{1}H NMR (500 MHz, $CDCl_3$, TMS): δ (ppm) 7.798 (br, 2H, −Ph), 7.708 (d, 2H, J = 16 Hz, −vinylic), 7.467 (br, 4H, −Ph), 6.642 (s, 2H, −PM), 6.548 (d, 2H, J = 16 Hz, −vinylic), 2.792 (br, 4H, $-\alpha CH_2$), 2.667 (br, 4H, $-\alpha CH_2$), 2.036 (br, 4H, $-\alpha CH_2$), 1.095−1.645 (m, 48H, $-CH_2$), 0.881 (br, 12H, $-CH_3$), 0.812 (t, 12H, J = Hz, $-CH_3$). ^{13}C NMR (125 MHz, $CDCl_3$, TMS): δ (ppm) 158.679, 155.899, 151.829, 147.352, 142.750, 141.025, 140.260, 133.847, 129.179, 129.010, 128.931, 128.685, 128.435, 123.831, 120.600, 120.404, 120.332, 116.483, 115.991, 107.082, 106.907, 59.133, 55.789, 40.900, 32.340, 32.233, 32.092, 32.020, 31.335, 30.499, 30.017, 29.961, 29.472, 28.324, 27.986, 25.365, 24.394, 23.102, 23.001, 14.449. Elem. Anal. Calcd for $C_{69}H_{90}N_2OS_2$: C, 80.65; H, 8.77. Found: C, 80.99; H, 9.08.

Poly{(10-hexyl-10*H*-phenothiazine-3,7-ylene)-*alt*-2-(2,6-bis((*E*)-2-(5-bromo-3,4-dihexylthiophen-2-yl)vinyl)-4*H*-pyran-4-ylidene)malononitrile} (PPTMT). The resulting polymer PPTMT was obtained as a dark green shining powder with a yield of 74%. ^{1}H NMR (500 MHz, $CDCl_3$, TMS): δ (ppm) 7.643 (d, 2H, J = 15.5 Hz, −vinylic), 7.225 (br, 4H, −Ph), 6.921 (br, 2H, −Ph), 6.603 (s, 2H, −PM), 6.467 (d, 2H, J = 15.5 Hz, −vinylic), 3.913 (br, 2H, $-\alpha CH_2$), 2.730 (br, 4H, $-\alpha CH_2$), 2577 (br, 4H, $-\alpha CH_2$), 1.885 (br, 2H, $-CH_2$), 1.588 (br, 4H, $-CH_2$), 1.493 (br, 6H, $-CH_2$), 1.288−1.421 (m, 28H, $-CH_2$), 0.869 (m, 15H, $-CH_3$). ^{13}C NMR (125 MHz, $CDCl_3$, TMS): δ (ppm) 158.238, 155.492, 146.879, 144.602, 140.621, 139.736, 133.188, 128.722, 128.274, 127.718, 124.407, 115.962, 115.620, 115.278, 106.470, 58.583, 47.777, 31.887, 31.775, 31.647, 31.426, 30.794, 29.707, 29.545, 29.368, 28.946, 27.849, 27.273, 26.953, 26.841, 22.667, 22.598, 14.077, 14.018. Elem. Anal. Calcd for $C_{62}H_{77}N_3OS_3$: C, 76.26; H, 7.89. Found: C, 77.03; H, 8.21.

Poly{(2,2′-bithiophene-5,5′-ylene)-*alt*-2-(2,6-bis((*E*)-2-(5-bromo-3,4-dihexylthiophen-2-yl)vinyl)-4*H*-pyran-4-ylidene)malononitrile} (PDTTMT). The resulting polymer PDTTMT was obtained as a dark powder with a yield of 52%. ^{1}H NMR (500 MHz, $CDCl_3$, TMS): δ (ppm) 7.601 (d, 2H, J = 15.0 Hz, −vinylic), 7.158 (br, 4H, −Th), 6.594 (s, 2H, −PM), 6.453 (d, 2H, J = 15.5 Hz, −vinylic), 2.722 (br, 8H, $-\alpha CH_2$), 1.582 (br, 8H, $-CH_2$), 1.357 (br, 24H, $-CH_2$), 0.928 (br, 6H, $-CH_3$), 0.866 (br, 6H, $-CH_3$). ^{13}C NMR (125 MHz, $CDCl_3$, TMS): δ (ppm) 158.168, 155.648, 147.586, 145.408, 143.836, 140.886, 138.711, 134.329, 130.145, 128.415, 124.850, 117.112, 115.773, 107.134, 59.745, 32.131, 32.035, 31.955, 30.780, 29.885, 29.724, 28.834, 28.480, 28.146, 23.043, 14.484, 14.428. Elem. Anal. Calcd for $C_{52}H_{62}N_2OS_4$: C, 72.69; H, 7.22. Found: C, 72.86; H, 7.36.

Characterization. The infrared spectra were recorded via the KBr pellet method by using a Nicolet Impact 410 FT-IR spectrophotometer. The elemental analysis was carried out with a Thermoquest CHNS-Ovelemental analyzer. The gel permeation chromatographic (GPC) analysis was carried out with a Waters 410 instrument with tetrahydrofuran as the eluent (flow rate: 1 mL/min, at 35 °C) and polystyrene as the standard. Differential scanning calorimetry (DSC) were performed under nitrogen flushing at a heating rate of 20 °C/min with a NETZSCH (DSC-204) instrument. Thermogravimetric analysis were performed on a Perkin-Elmer Pyris 1 analyzer under a nitrogen atmosphere (100 mL/min) at a heating rate of 10 °C/min. ^{1}H NMR and ^{13}C NMR spectra were measured using a Bruker AVANCE-500 NMR spectrometer spectrometer and a Varian Mercury-300 NMR, respectively. UV−vis absorption spectra were measured using a Shimadzu UV-3100 spectrophotometer. The photoluminescenece spectra of spin-cast films and solution were measured with a RF-5301PC spectrofluorophotometer. Electrochemical measurements of these derivatives were performed with a Bioanalytical Systems BAS 100 B/W electrochemical workstation. Atomic force microscopy (AFM) images of blend films were carried out using a Nanoscope IIIa Dimension 3100.

Photovoltaic Device Fabrication and Characterization. For device fabrication, the ITO glass was precleaned and modified by a thin layer of PEDOT:PSS, which was spin-cast from a PEDOT:PSS aqueous solution (H.C. Starck) on the ITO

Scheme 1. Synthetic Routes of the Monomers

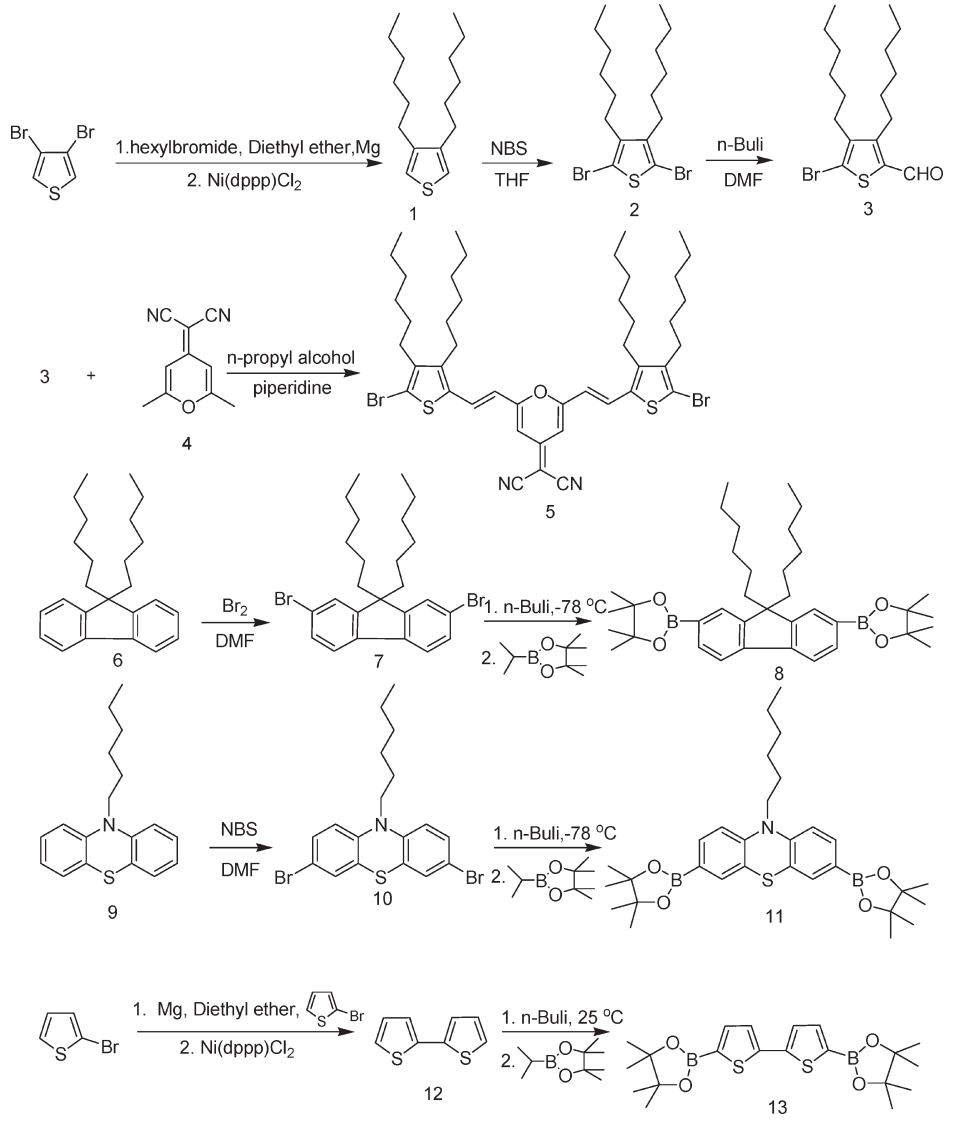

substrate, and the thickness of the PEDOT:PSS layer is about 50 nm. The active layer contained a blend of copolymers as electron donor and PCBM as electron acceptor, which was prepared from a 1:3 by weight solution (8 mg/mL) in chlorobenzene for PFTMT and PPTMT and chloroform for PDTTMT. After spin-coating the blend from solution at 2500 rpm, the devices were completed by evaporating a 0.6 nm LiF layer protected by 100 nm of Al at a base pressure of 5×10^{-4} Pa. The effective photovoltaic area as defined by the geometrical overlap between the bottom ITO electrode and the top cathode was 4 or 5 mm^2. The thickness of the photoactive layer was 50−60 nm, measured by the Ambios Technology XP-2. The current−voltage ($I-V$) characterization of PV devices in the dark and under white-light illumination from a SCIENCETECH 500 W solar simulator (AM 1.5 100 mW/cm^2) were measured on computer-controlled Keithley 2400 Source Meter measurement system. All the measurements were performed under ambient atmosphere at room temperature.

Results and Discussion

Material Synthesis and Structural Characterization. The general synthetic routes toward the monomers are outlined in Scheme 1. In the first step, 3,4-dihexylthiophene (**1**) was synthesized from 3,4-dibromothiophene by nickel-catalyzed cross-coupling with bromohexylmagnesium reagent.[19] Bromination of **1** by *N*-bromosuccinimide (NBS) gave the dibromo compound (**2**) in high yield. Critical to the synthetic strategy was the selective halogen−metal exchange followed by conversion to the aldehyde. The monoaldehyde of 2,5-dibromo-3,4-dihexylthiophene (**2**) was prepared by a modified procedure with 1.1 equiv of *n*-BuLi followed by DMF. The monomer (**5**) was prepared through Knoevenagel condensation of 2-(2,6-dimethypyran-4-ylidene)malomonitrile (**4**) with 5-bromo-3,4-dihexylthiophene-2-carbaldehyde (**3**). The structures of monomer (**5**) were confirmed by ^1H NMR, ^{13}C NMR, and elemental analysis, and the data are included in the Experimental Section. In ^1H NMR spectroscopy of monomer (**5**), the coupling constant ($J \sim 15.5$ Hz) of olefinic protons indicates that the Knoevenagel reaction afforded the pure all-trans isomers, which is further confirmed by the characterization of vibration band of trans double bond at 960 cm^{-1} in the FT-IR spectra (see Supporting Information). 2,7-Bis(4,4,5,5-tetramathyl-1,3,2-dioxaborolan-2-yl)-9,9-dihexylfluorene (**8**) and 10-hexyl-3,7-bis(4,4,5,5-tetramethyl-1,3,2-dioxaborolan-2-yl)-10*H*-phenothiazine (**11**) as well as 5,5′-bis(4,4,5,5-tetramethyl-1,3,2-dioxaborolan-2-yl)-2,2′-bithiophene (**13**) were prepared according to previously reported methods.[20−22] The

Scheme 2. Synthetic Routes of the Polymers

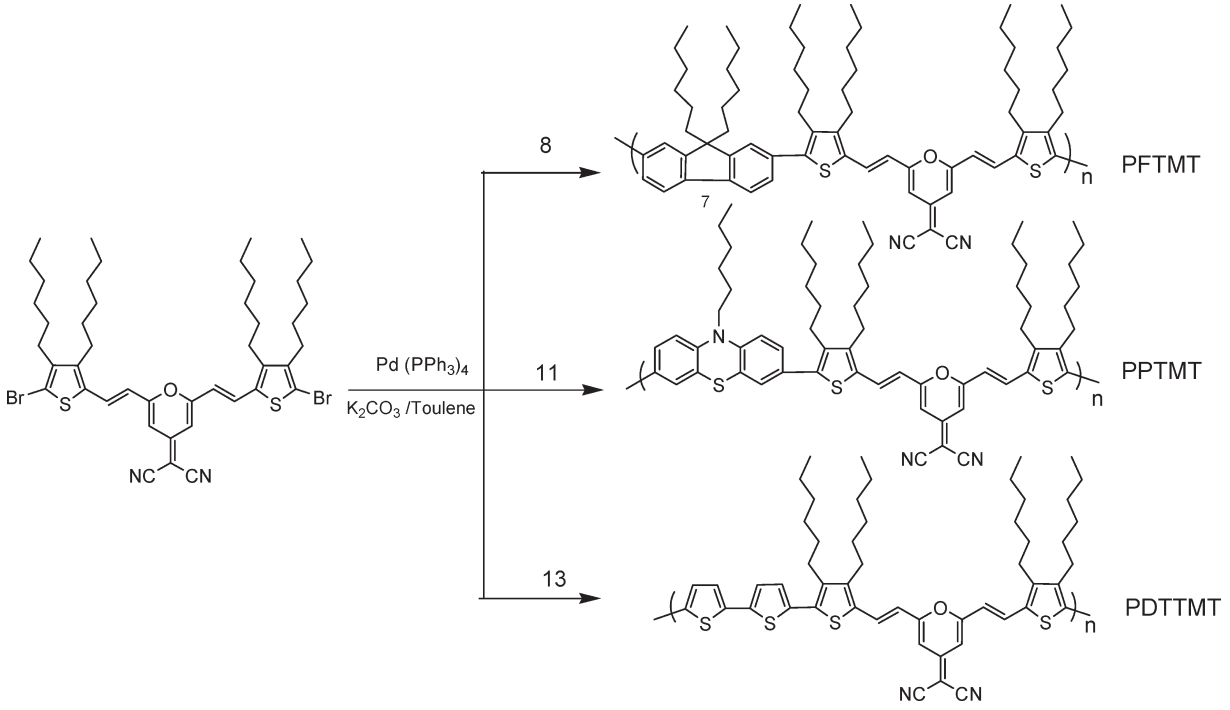

polymerization reaction was proceeded by the well-known palladium-catalyzed Suzuki coupling reaction between varied bis-trimethyleneborate monomers (**8**, **11**, **13**) and functionalized dibromo aromatic monomer **5**.[23] The synthetic routes of polymers are shown in Scheme 2. The ^{1}H NMR and ^{13}C NMR spectra of PFTMT and their assignments shown in Figure 1 are consistent with the proposed structure. NMR spectra clearly indicate that well-defined PFTMT has been obtained. The two legible double peaks that appear at 6.548 and 7.708 ppm with the coupling constant ($J \sim 16$ Hz) are due to the all-trans double bond, which further confirms the regular structure. The NMR spectra of other polymers also showed a good agreement with the proposed polymer structures.

All the polymers exhibited excellent solubility in common organic solvents such as chloroform, tetrahydrofuran, dichloromethane, and chlorobenzene. Molecular weights and polydispersities of the resulting polymers were determined by GPC analysis with the number-average molecular weight (M_n) of 5700−43 800 and PDI (polydispersity index, M_w/M_n) of 1.02−4.59. Table 1 summarizes the polymerization results including molecular weights, PDI, and thermal stability of the polymers. The bithiophene without alkylation, which prevented the polymerization due to its low solubility, should be the main reason for the low polymerization of PDTTMT. The large polydispersity in the molecular weight of PFTMT and PPTMT may be a result of the precipitation of polymer from the reaction solution.

Thermal Properties. All the polymers exhibited good thermal stability with 5% weight-loss temperatures (T_d) higher than 296 °C under N_2 and high glass transition temperatures (T_g) of 112−130 °C, as revealed by thermogravimetric analysis (TGA) and the differential scanning calorimetry (DSC), respectively (see Figure 2). The high thermal stability of the resulting polymers prevents the deformation of the polymer morphology and the degradation of active layer applied in PVCs.

Optical Properties. The normalized UV−vis absorption spectra of PFTMT, PPTMT, and PDTTMT in dilute chloroform solution (concentration 10^{-5} M) are shown in Figure 2, and the main optical properties are listed in Table 2. PFTMT with the weak electron-donating dialkyfluorene moiety showed two absorption bands at 332 and 483 nm in dilute solution (Figure 2a), which can be assigned to $\pi-\pi^*$ transition of the conjugated polymer backbone and ICT interaction between the fluorene donor and TVM-based acceptor. Similarly, the absorption spectra of other copolymers (PPTMT and PDTTMT) in dilute solutions showed also two bands near 330 and 500 nm due to the $\pi-\pi^*$ transition and the ICT interaction. The solution absorption spectrum of PDTTMT, with an absorption maximum (λ_{max}^{abs}) at 500 nm and the absorption edge (λ_{edge}) at 636 nm, is broadened and red-shifted compared to those of PFTMT (λ_{max}^{abs} = 483 nm, λ_{edge} = 568 nm) and PPTMT (λ_{max}^{abs} = 494 nm, λ_{edge} = 592 nm), which can be explained by much stronger ICT effect in the PDTTMT than that in PFTMT and PPTMT. Among these three copolymers, there is an alternating "D*−(D−A−D)" structure, where the D* is the donor with varied electron-donating ability and D−A−D is the TVM-based acceptor unit which is consist of the unchangeable donor D (2,5-linked thiophenevinyl) and acceptor A (2-pyran-4-ylidenemalononitrile). The stronger electron-donating ability D* possesses, the higher electronic delocalization degree and the stronger ICT the copolymer has. Since the order of the electron-donating abilities of the three D* is bithiophene > alkylphenothiazine > dialkylfluorene, the strongest electron-donating ability of bithiophene compared to dialkylfluorene and alkylphenothiazine improves the effective conjugation length along polymer backbone, resulting in an increase in the ICT strength and thus electronic delocalization.[24] Moreover, the relatively high absorption coefficients (ε_{max}) could be calculated from Beer's law equation with the same dilute concentration of the copolymers in chloroform, which assures the copolymers can absorb enough photons.

Figure 2b shows the optical absorption spectra of thin films of the copolymers. The thin film absorption spectra are generally similar in shape to those in dilute solution, The

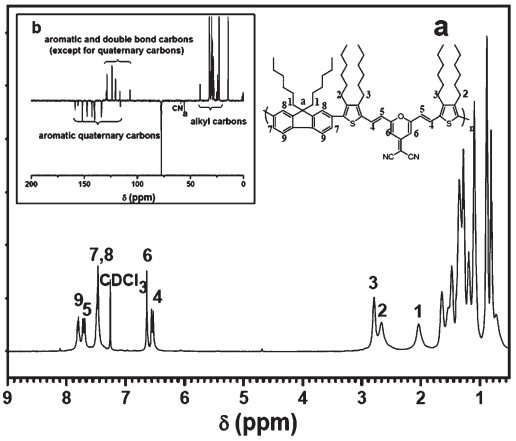

Figure 1. (a) ^{1}H NMR spectrum and chemical structure of PFTMT in $CDCl_3$ solution. (b) ^{13}C NMR spectrum of PFTMT in $CDCl_3$ solution.

Table 1. Polymerization Results for Copolymers PFTMT, PPTMT, and PDTTMT

	M_n (kg/mol)[a]	M_w (kg/mol)[a]	PDI	T_g[b] (°C)	T_d[c] (°C)
PFTMT	43.8	183.8	4.20	115	380
PPTMT	31.6	145.1	4.59	130	384
PDTTMT	5.7	5.9	1.04	112	296

[a] Calculated from GPC (eluent: THF; polystyrene standards). [b] Determined by DSC at a heating rate of 20 °C/min under nitrogen. [c] Temperature at 5% weight loss by a heating rate of 10 °C/min under nitrogen.

absorption peaks of PFTMT and PPTMT show no significant difference between in solutions and thin films, which can be explained by their nonplanar conformations due to the fluorene and phenothiazine moieties, and their long alkyl side chains can induce the twist of the copolymer backbone, which is harmful to the $\pi-\pi$ stacking in the solid state.[25] It should be noted that the absorption edge of PPTMT in thin film exhibits a 58 nm red shift compared to that in solution, while PFTMT only shows 13 nm red shift. The larger red shift of the absorption edge for PPTMT may be caused by less alkyl side chains of phenothiazine and an increase in conjugation length of PPTMT backbone resulting from a more planar conformation in the solid state compared to that in solution, which can lead to more efficient $\pi-\pi$ stacking.[26] In the case of PDTTMT, the absorption peak in the solid state exhibits a relatively large red shift of 49 nm, and the red shift of the absorption edge is 67 nm compared to that in solution, possibly assisted by planarization and the increase of conjugation length.[27] The high coplanarity of PDTTMT, which leads to a great improvement $\pi-\pi$ stacking, is mainly caused by the symmetrical coplanar TVM and essentially planar bithiophene group in the solid state.[28] However, the low coplanarities of PFTMT and PPTMT are obtained due to the incorporating nonplanar fluorene and phenothiazine moieties.[29]

The ICT absorption bands of the three copolymers are tuned from 483 to 549 nm, and the optical band gap $E_{g,opt}$ of the copolymers derived from the absorption edge of the thin film spectra is in the range of 2.13−1.76 eV (Table 2). As expected, among the three copolymers, PDTTMT with the strongest intramolecular charge transfer interaction thus has the lowest optical band gap of 1.76 eV, which is 0.24 eV lower than that of poly(3-alkylthiophene) homopolymer (~2.0 eV).[30] It is evident that the ICT interaction between donor and acceptor moieties in D−A copolymers is a practical approach to lower the band gap and broaden the

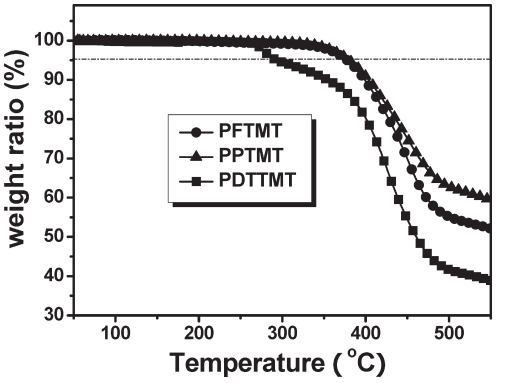

Figure 2. TGA thermograms of the copolymers.

absorption bands across the entire visible wavelength region of conjugated polymers.[31]

We also investigated the photoluminescence properties of the synthesized copolymers in solution and film (see Supporting Information). It has to be noted that all the polymers discussed here are poorly emissive except PFTMT in solution. The observed strong quenching of the luminescence is in good agreement with the occurrence of an ICT process.[32]

Electrochemical Properties. Figure 4 shows the cyclic voltammetry (CV) diagrams of the polymers using $TBAPF_6$ as supporting electrolyte in acetonitrile solution with platinum button working electrodes, a platinum wire counter electrode, and an $Ag/AgNO_3$ reference electrode under the N_2 atmosphere. Ferrocene was used as the internal standard. All the polymers showed reversible or partly reversible redox behavior, which was attributed to the high electrical activity. The onset oxidation potentials (E_{ox}^{onset}) of the three copolymers are observed in the range of 0.53−0.91 V. The onset reduction potentials (E_{red}^{onset}) are almost the same for the three copolymers (−1.16 V). The redox potential of Fc/Fc^+ which has an absolute energy level of −4.8 eV relative to the vacuum level for calibration is located at 0.08 V in 0.1 M $TBAPF_6$/acetonitrile solution.[33] So the evaluation of HOMO and LUMO levels as well as the band gap ($E_{g,ec}$) could be done according to the following equations:

$$\text{HOMO (eV)} = -e(E_{ox}^{onset} + 4.72)\ \text{(eV)}$$

$$\text{LUMO (eV)} = -e(E_{red}^{onset} + 4.72)\ \text{(eV)}$$

$$E_{g,ec} = E_{ox}^{onset} - E_{red}^{onset}\ \text{(eV)}$$

where E_{ox}^{onset} and E_{red}^{onset} are the measured potentials relative to Ag/Ag^+. The electrochemical properties as well as the energy level parameters of polymers are list in Table 2.

The estimated HOMO and LUMO energy levels of PFTMT are −5.63 and −3.57 eV, respectively. The LUMO energy levels of PPTMT and PDTTMT are −3.56 and −3.53 eV, which are very similar to that of PFTMT. Therefore, the substitution of D* with varied electron-donating ability moiety has almost no effect on the reduction potential of the copolymers. Besides, the relatively low LUMO energy levels of the three copolymers result from the stronger reduction of TVM-based acceptor unit. On the other hand, the HOMO energy levels of copolymers behave quite differently. The HOMO energy levels of the polymers PFTMT, PPTMT, and PDTTMT are in the range of −5.63 to −5.25 eV, which is clearly affected by the varied electron-donating ability of the three D* due to the modulation of the ICT

Table 2. Optical and Electrochemical Data of the Copolymers PFTMT, PPTMT, and PDTTMT

	in solution[a]		in film[b]					
polymer	λ_{max}^{abs}[nm] (ε_{max} [M^{-1} cm^{-1}])	λ_{edge} [nm]	λ_{max}^{abs} [nm]	λ_{edge} [nm]	E_{ox}^{onset} (V)/HOMO (eV)	E_{red}^{onset} (V)/LUMO (eV)	electrochem $E_{g,ec}$ (eV)	optical[c] $E_{g,opt}$ (eV)[c]
PFTMT	483 (49 270)	568	483	581	0.91/−5.63	−1.15/−3.57	2.06	2.13
PPTMT	494 (22 890)	592	494	650	0.53/-5.25	−1.16/−3.56	1.69	1.91
PDTTMT	500 (27 890)	636	549	703	0.57/-5.29	−1.19/−3.53	1.76	1.76

[a] 1×10^{-5} M in anhydrous chloroform. [b] Spin-coated from a 10 mg/mL chloroform solution. [c] The optical band gap ($E_{g,opt}$) was obtained from absorption edge.

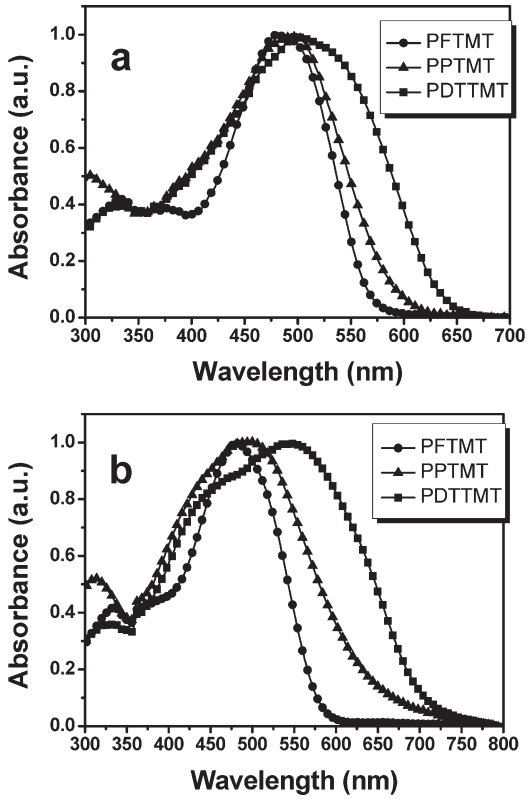

Figure 3. Normalized absorption spectra of the copolymers (a) in chloroform solutions with the concentration of 10^{-5} mol/L and (b) films spin-coated from a 10 mg/mL chloroform solution.

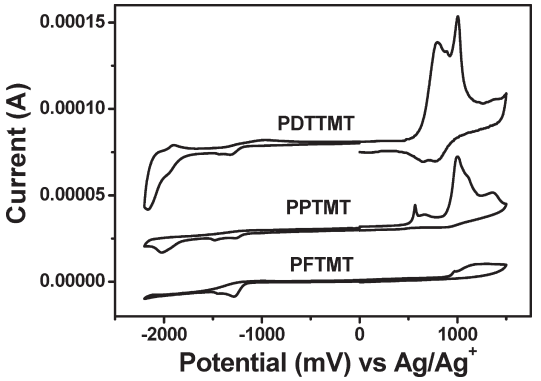

Figure 4. Cyclic volatammetry curves of PFTMT, PPTMT, and PDTTMT films on platinum electrode in 0.1 mol/L *n*-Bu_4NPF_6 in CH_3CN solution, at a scan rate of 100 mV/s.

strength. It is clear that both the HOMO levels of PPTMT (−5.25 eV) and PDTTMT (−5.29 eV) are higher than PFTMT (−5.63 eV), which caused by the stronger electron-donating ability of bithiophene and phenothiazine

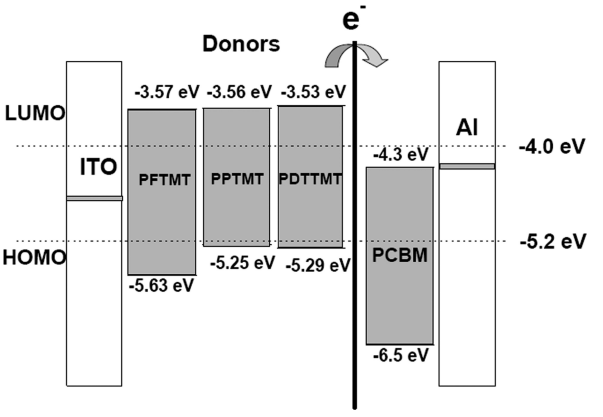

Figure 5. Band diagram for accepting PCBM and donor PFTMT, PPTMT, and PDTTMT polymers. Dashed lines indicate the thresholds for air stability (5.2 eV) and effective charge transfer PCBM (4.0 eV).

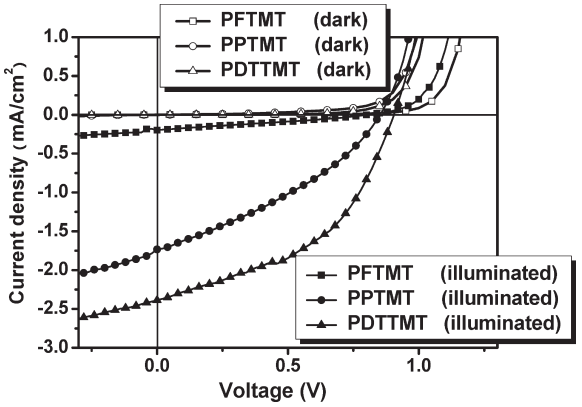

Figure 6. Current−voltage characteristics of polymer photovoltaic cells based on PFTMT, PPTMT, and PDTTMT in the dark and under illumination of AM 1.5, 100 mW/cm^2 white light.

compared to fluorene. However, compared with PDTTMT, PPTMT showed a similar HOMO energy level, which mainly caused by the electron-rich sulfur and nitrogen heteroatoms of phenothiazine that render the resulting conjugated backbone more electron-rich. Generally, the stronger electron-donating ability of D* resulted in a higher HOMO energy level.

The HOMO energy level of the donor polymers is very important for high performance photovoltaic cell. First, the polymers should have good air stability with HOMO energy level being below the air oxidation threshold (ca. −5.2 eV).[34] Second, the relatively low HOMO level of the polymers can allow a high open-circuit potential (V_{oc}) value for the photovoltaic cell.[25] A complete picture of the band structure of the copolymers is presented in Figure 5. The first dashed line indicates the threshold for air stability, and the second dashed line represents the threshold value for an effective

Table 3. Characteristic Current−Voltage Parameters from Device Testing at Standard AM 1.5G Conditions and Blend Films Roughness of AFM Measurement

	polymer/PCBM (w/w ratio)	V_{oc} (V)[a]	J_{sc} (mA/cm^2)[a]	FF[a]	rms (nm)[b]	PCE (%)[a]
PFTMT	1:3	0.80	0.20	0.28	5.73	0.04
PPTMT	1:3	0.86	1.73	0.34	1.17	0.51
PDTTMT	1:3	0.90	2.39	0.46	1.64	0.99

[a] Photovoltaic properties of copolymer/PCBM-based devices spin-coated from a chlorobenzene solution for PFTMT (1:3 w/w), PPTMT (1:3 w/w), and from a chloroform solution for PDTTMT (1:3 w/w). [b] Root mean-square (rms) roughness from AFM measurement.

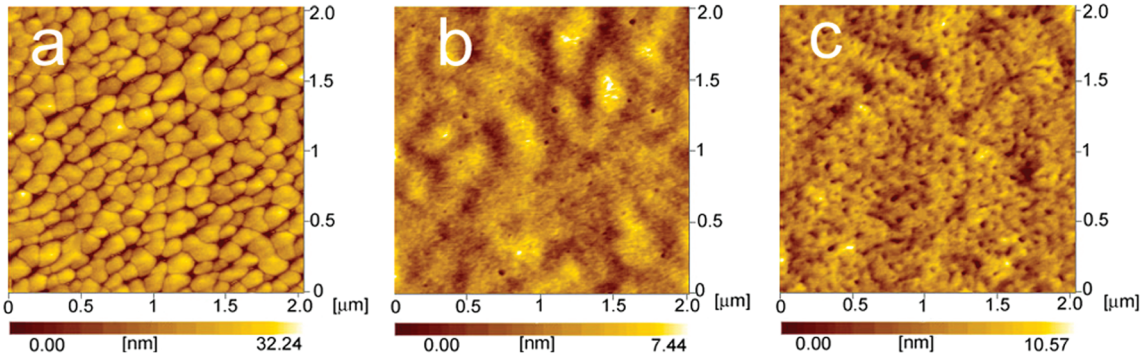

Figure 7. Topography image (size 2 μm × 2 μm) obtained by tapping-mode AFM showing the morphology of the blend films spin-coated from chlorobenzene for PFTMT and PPTMT and chloroform for PDTTMT: (a) PFTMT/PCBM (w/w, 1:3); (b) PPTMT/PCBM (w/w, 1:3); (c) PDTTMT/PCBM (w/w, 1:3).

charge transfer from the polymers to PCBM (−4.0 eV).[34b] Both the HOMO energy levels and LUMO energy levels of the copolymers are in the ideal range. It is worth noting that the electrochemical band gap ($E_{g,ec}$) and optical band gap ($E_{g,opt}$) are relatively in good agreement for the copolymers. The varied HOMO energy level and relative stable LUMO energy level result in the reduced band gaps of the copolymers, which also demonstrates the significance of the intramolecular charge transfer through the D−A structures inside the copolymers. So, the HOMO energy level and band gap of the copolymers can be controlled strictly by introducing different electron-donating ability electron donors.

Photovoltaic Properties. In order to investigate the photovoltaic properties of the copolymers, the BHJ photovoltaic cells with a structure of ITO/PEDOT−PSS/copolymers: PCBM/LiF/Al were fabricated, where the copolymers were used as donors and PCBM as acceptor.[35] It is known that solvents used for the preparation of the active layer have a strong impact on the performance of the cell.[36] Here, we chose chlorobenzene for PFTMT and PPTMT, and chloroform was chosen for PDTTMT in order to obtain the films with the relative good quality. The devices were characterized in the dark and under solar simulator AM1.5 (100 mW/cm^2) with simultaneous recording of their current−voltage characteristics. The current−voltage characteristics of the photovoltaic cell based on PFTMT:PCBM, PPTMT:PCBM, and PDTTMT:PCBM with weight ratio (1:3 w/w) are presented in Figure 6. The photovoltaic parameters of the photovoltaic cells are summarized in Table 3.

The cell based on PFTMT:PCBM (1:3 w/w) showed an open-circuit voltage (V_{oc}) of 0.80 V, a short-circuit current (J_{sc}) of 0.20 mA/cm^2, and a fill factor (FF) of 0.28, giving a power conversion efficiency (PCE) of 0.04%. The low J_{sc} of the cell may be caused by the weak ICT interaction inside PFTMT and the bad aggregated configuration in solid state of PFTMT:PCBM blend film which leads to the low absorption of solar spectrum and hindered charge transport. However, greatly enhanced device performance was obtained for the other two cells based on PPTMT:PCBM (1:3 w/w) and PDTTMT:PCBM (1:3 w/w) with V_{oc} of 0.86 and 0.90 V, J_{sc} of 1.73 and 2.39 mA/cm^2, FF of 0.34 and 0.46, and PCE of 0.51% and 0.99%, respectively. The reason for the improvement PCE could be explained by the strong ICT interaction and better $\pi-\pi$ stacking of PPTMT and PDTTMT in the solid state.

Film morphology of the active layer, i.e., the blend film of the donor polymer and the acceptor (e.g., PCBM), has been found to be one of the key elements in determining the PCE of polymer photovoltaic cell.[37] Figure 7a−c shows the AFM height images of PFTMT:PCBM, PPTMT:PCBM, and PDTTMT:PCBM blend films with the same weight ratio (1:3 w/w) for effective comparison and further elucidation of the difference in PVCs performance. As is clearly evidenced by AFM, the PFTMT:PCBM blend film shows a most coarse surface with the root-mean-square (rms) of 5.73 nm (Figure 7a and Table 3), and obvious PCBM grain-aggregation with the size distribution around 150 nm is almost homogeneously dispersed in the PFTMT matrix, which may result in a large-scale phase separation, decreased diffusional escape probability for mobile charge carriers, and hence increased recombination. This is fully consistent with the relative low short-circuit densities obtained for the PFTMT:PCBM cell (0.20 mA/cm^2). Compared with the PFTMT/PCBM blend film, PPTMT:PCBM blend film shows a flat surface with the rms of 1.17 nm (Figure 7b), and no obvious phase separation is observed. Since PPTMT and PCBM molecules have good miscibility, increased interfacial area is expected, and the J_{sc} of PPTMT:PCBM (1:3 w/w) based device increases to 1.73 mA/cm^2, which is nearly 8 times higher than that of PFTMT:PCBM based device. In the case of PDTTMT:PCBM blend film (Figure 7c), it shows uniform phase separation. The formation of PDTTMT-rich islands can be seen more clearly, whereas for the other two polymers, these morphological features are not observed. The formation of these self-organized aggregates of PDTTMT via $\pi-\pi$ stacking interactions (whose evidence could also be found in the specific features of the absorption spectra of the polymer thin films) as well as the broad and strong absorption of the PDTTMT:PCBM based device

should be responsible for the increase of the short-circuit densities (up to 2.38 mA/cm^2). Furthermore, as discussed above, the V_{oc} is directly governed by the difference between the HOMO energy levels of the donor and the LUMO of the acceptor. However, several other parameters must be taken into account such as carrier recombination, resistance related to thickness of the active layer, and degree of phase separation between the components in the blend, which can modify the energetically expected V_{oc} value. Therefore, although the HOMO energy level of PFTMT is the highest among the three polymers, the V_{oc} value of PFTMT-based device was lower than PPTMT and PDTTMT-based devices. The relative low V_{oc} (0.80 V) for PFTMT based device could be explained by the large numbers of carrier recombination due to the obvious grain-aggregation and large-scale blend phase separation. But all the other two copolymers have a satisfying V_{oc} (around 0.90 V), which is much higher than the P3HT:PCBM-based device (0.6 V).[38]

As discussed above, the photovoltaic properties of TVM-based copolymers incorporating varied electron-donating and coplanarity moiety D* were greatly improved with the increasing of ICT bands and $\pi-\pi$ stacking in solid state. It is a prominent found in the molecular design of PDTTMT: broad absorption (350−700 nm), high V_{oc} (0.90 V), and the best tuned PCE value of 0.99%. The PCE of PDTTMT is more than 23 times higher than that obtained from PFTMT (PCE = 0.04%). All the devices of the copolymers were prepared and characterized in air, without protecting environment, which demonstrated the high stability of the polymers. The corresponding low FF values suggested that there is still considerable room for future improvement in the device performance through optimization of the device structure. Using the design rules proposed by Brabec et al.,[39] which assume a charge carrier mobility of 10^{-3} cm^2 V^{-1} s^{-1}, a fill factor of 0.65, and an optimal morphology, one can estimate the overall power conversion efficiency from the optical band gap and the offset values between the LUMO levels of donors and acceptor. This model predicts that PDTTMT can expect a power conversion efficiency over 5%.

Conclusions

We have designed and synthesized three novel π-conjugated copolymers consisting of TVM-based unit coupled to different electron-donating ability moieties by Suzuki coupling polymerization. Optical property investigations unequivocally indicate that these new copolymers exhibit enhanced $\pi-\pi$ stacking and ICT bands in solid state by changing the macromolecular architecture, which lead to an extension of their absorption spectral range. The copolymers had optical band gaps in the range of 1.76−2.13 eV. The HOMO and LUMO energy levels of resulting copolymers can be fine-tuned as demonstrated from the investigation of electrochemical study. The relatively low HOMO energy levels promised good air stability and high V_{oc} for photovoltaic cells application. The highest PCE value of 0.99% was obtained from the device based on PDTTMT with a strongest electron-donating ability D*, which was more than 23 times higher than that of the device based on PFTMT (0.04%). Although the power conversion efficiencies for these unoptimized photovoltaic devices are still not sufficiently high, their tunable electronic properties provide an understanding on how the polymer structures affect the device characteristics. Further optimization on the photovoltaic cell structure (such as film thickness or electrode materials) or processing conditions (such as annealing) could lead to enhanced efficiency of photovoltaic cells.

Acknowledgment. This work was supported by the State Key Development Program for Basic Research of China (Grant 2009CB623605), the National Natural Science Foundation of China (Grants 50673035, 20874035), Program for New Century Excellent Talents in Universities of China Ministry of Education, the 111 Project (Grant B06009), and the Project of Jilin Province (Grant 20080305).

Supporting Information Available: Experimental details of the synthesis of the polymers; ^{1}H and ^{13}C NMR spectra of compound **3**, monomer **5**, **11**, **13**; FT-IR spectra of monomer **5**; photoluminescence spectra of the copolymer in solution and film. This material is available free of charge via the Internet at http://pubs.acs.org.

References and Notes

(1) (a) Yu, G.; Gao, J.; Hummelen, J. C.; Wudl, F.; Heeger, A. J. *Science* **1995**, *270*, 1789–1791. (b) Gunes, S.; Neugebauer, H.; Sariciftci, N. S. *Chem. Rev.* **2007**, *107*, 1324–1338.
(2) (a) Chen, C. P.; Chan, S. H.; Chao, T. C.; Ting, C.; Ko, B. T. *J. Am. Chem. Soc.* **2008**, *130*, 12828–12833. (b) Blouin, N.; Michaud, A.; Gendron, D.; Wakim, S.; Blair, E.; Plesu, R. N.; Bellette, M.; Durocher, G.; Tao, Y.; Leclerc, M. *J. Am. Chem. Soc.* **2008**, *130*, 732–742.
(3) Chang, Y. T.; Hsu, S. L.; Chen, G. Y.; Su, M. H.; Singh, T. A.; Diau, E. W. G.; Wei, K. H. *Adv. Funct. Mater.* **2008**, *18*, 2356–2365.
(4) Liang, Y. Y.; Wu, Y.; Feng, D. Q.; Tsai, S. T.; Son, H. J.; Li, G.; Yu, L. P. *J. Am. Chem. Soc.* **2009**, *131*, 56–57.
(5) Sacriciftci, N. S.; Smilowitz, L.; Heeger, A. J.; Wudl, F. *Science* **1992**, *258*, 1474–1476.
(6) (a) Li, G.; Shrotriya, V.; Huang, J. S.; Yao, Y.; Moriarty, T.; Emery, K.; Yang, Y. *Nat. Mater.* **2005**, *4*, 864–868. (b) Ma, W. L.; Yang, C. Y.; Gong, X.; Lee, K. H.; Heeger, A. J. *Adv. Funct. Mater.* **2005**, *15*, 1617–1622.
(7) Coakley, K. M.; McGehee, M. D. *Chem. Mater.* **2004**, *16*, 4533–4542.
(8) (a) van Mullekom, H. A. M.; Vekemans, J. A. J. M.; Havinga, E. E.; Meijer, E. W. *Mater. Sci. Eng. R* **2001**, *32*, 1–40. (b) Tsai, F. C.; Chang, C. C.; Liu, C. L.; Chen, W. C.; Jenekhe, S. A. *Macromolecules* **2005**, *38*, 1958–1966.
(9) (a) Neef, C. J.; Brotherston, I. D.; Ferraris, J. P. *Chem. Mater.* **1999**, *11*, 1957–1958. (b) Lee, K.; Sotzing, G. A. *Macromolecules* **2001**, *34*, 5746–5747. (c) Campos, L. M.; Tontcheva, A.; Gunes, S.; Sonmez, G.; Neugebauer, H.; Sariciftci, N. S.; Wudl, F. *Chem. Mater.* **2005**, *17*, 4031–4033.
(10) (a) Zhang, F. L.; Mammo, W.; Andersson, L. M.; Admassie, S.; Andersson, M. R.; Inganas, L.; Admassie, S.; Andersson, M. R.; Ingands, O. *Adv. Mater.* **2006**, *18*, 2169–2173. (b) Blouin, N.; Michaud, A.; Leclerc, M. *Adv. Mater.* **2007**, *19*, 2295–2300. (c) Wong, W. Y.; Wang, X. Z.; He, Z.; Djurisic, A. B.; Yip, C. T.; Cheung, K. Y.; Wang, H.; Mak, C. S. K.; Chan, W. K. *Nat. Mater.* **2007**, *6*, 521–527.
(11) Halls, J. J. M.; Pichler, K.; Friend, R. H.; Moratti, S. C.; Holmes, A. B. *Appl. Phys. Lett.* **1996**, *68*, 3120–3122.
(12) Chan, S. H.; Chen, C. P.; Chao, T. C.; Ting, C.; Lin, C. S.; Ko, B. T. *Macromolecules* **2008**, *41*, 5519–5526.
(13) Leclerc, N.; Michaud, A.; Sirois, K.; Morin, J. F.; Leclerc, M. *Adv. Funct. Mater.* **2006**, *16*, 1694–1704.
(14) (a) Lee, S. K.; Jung, B. J.; Ahn, T.; Jung, Y. K.; Lee, J. I.; Kang, I. N.; Lee, J.; Park, J. H.; Shim, H. K. *J. Polym. Sci., Part A: Polym. Chem.* **2007**, *45*, 3380–3390. (b) He, C.; He, Q. J.; Yang, X. D.; Wu, J. L.; Yang, C. H.; Bai, F. L.; Shuai, Z. G.; Wang, L. X.; Li, Y. F. *J. Phys. Chem. C* **2007**, *111*, 8661–8666.
(15) Anuragudom, P.; Newaz, S. S.; Phanichphant, S.; Lee, T. R. *Macromolecules* **2006**, *39*, 3494–3499.
(16) Kong, X. X.; Kulkarni, A. P.; Jenekhe, S. A. *Macromolecules* **2003**, *36*, 8992–8999.
(17) Woods, L. L. *J. Am. Chem. Soc.* **1958**, *80*, 1440–1442.
(18) Kagan, J.; Arora, S. K. *J. Org. Chem.* **1983**, *48*, 4317–4320.
(19) Tamao, K.; Odama, S.; Nakasima, I.; Kumada, M.; Minato, A.; Suzuki, K. *Tetrahedron* **1982**, *38*, 3347–3354.
(20) Ranger, M.; Rondeau, D.; Leclerc, M. *Macromolecules* **1997**, *30*, 7686–7691.
(21) Sailer, M.; Gropeanu, R.-A.; Muller, T. J. J. *J. Org. Chem.* **2003**, *68*, 7509–7512.

(22) Melucci, M.; Barbarella, G.; Sotgiu, G. *J. Org. Chem.* **2002**, *67*, 8877–8884.
(23) Burn, P. L.; Holmes, A. B.; Kraft, A.; Bradley, D. D. C.; Brown, A. R.; Friend, R. H.; Gywer, R. W. *Nature (London)* **1992**, *356*, 47–49.
(24) Wu, P. T.; Kim, F. S.; Champion, R. D.; Jenekhe, S. A. *Macromolecules* **2008**, *41*, 7021–7028.
(25) Li, Y. W.; Xue, L. L.; Xia, H. J.; Xu, B.; Wen, S. P.; Tian, W. J. *J. Polym. Sci., Part A: Polym. Chem.* **2008**, *46*, 3970–3984.
(26) Zhu, Y.; Babel, A.; Jenekhe, S. A. *Macromolecules* **2005**, *38*, 7983–7991.
(27) Apperloo, J. J.; Janssen, R. A. J.; Malenfant, P. R. L.; Frechet, J. M. J. *Macromolecules* **2000**, *33*, 7038–7043.
(28) Devi, L. S.; Al-Suti, M. K.; Zhang, N.; Teat, S. J.; Male, L.; Sparkes, H. A.; Raithby, P. R.; Khan, M. S.; Kohler, A. *Macromolecules* **2009**, *42*, 1131–1141.
(29) (a) Marcon, V.; Vegt, N. V. D.; Wegner, G.; Raos, G. *J. Phys. Chem. B* **2006**, *110*, 5253–5261. (b) Yang, L.; Feng, J. K.; Ren, A. M. *J. Org. Chem.* **2005**, *70*, 5987–5996.
(30) (a) Chen, T. A.; Wu, X.; Rieke, R. D. *J. Am. Chem. Soc.* **1995**, *117*, 233–244. (b) Babel, A.; Jenekhe, S. A. *J. Phys. Chem. B* **2003**, *107*, 1749–1754.
(31) (a) Campos, L. M.; Tontcheva, A.; GUnes, S.; Sonmez, G.; Neugebauer, H.; Sariciftci, N. S.; Wudl, F. *Chem. Mater.* **2005**, *17*, 4031–4033. (b) Svensson, M.; Zhang, F.; Veenstra, S. C.; Verhees, W. J. H.; Hummelen, J. C.; Kroon, J. M.; Inganas, O.; Andersson, M. R. *Adv. Mater.* **2003**, *15*, 988–991. (c) Wu, P. T.; Kim, F. S.; Champion, R. D.; Jenekhe, S. A. *Macromolecules* **2008**, *41*, 7021–7028.
(32) Sophie, R.; Antonio, C.; Philippe, L.; Olivier, A.; Pierre, F.; Jean, R. *J. Am. Chem. Soc.* **2006**, *128*, 3459–3466.
(33) (a) Pommerehne, J.; Vestweber, H.; Guss, W.; Mahrt, R. F.; Bassler, H.; Porsch, M.; Daub, J. *Adv. Mater.* **1995**, *7*, 551–554. (b) Zhou, Y. H.; Peng, P.; Han, L.; Tian, W. J. *Synth. Met.* **2007**, *157*, 502–507.
(34) (a) Leeuw, D. M. D.; Simenon, M. M. J.; Brown, A. R.; Einerhand, R. E. F. *Synth. Met.* **1997**, *87*, 53–59. (b) Thompson, B. C.; Kim, Y. G.; Reynolds, J. R. *Macromolecules* **2005**, *38*, 5359–5362.
(35) Li, G.; Shrotriya, V.; Huang, J.; Yao, Y.; Moriarty, T.; Emery, K.; Yang, Y. *Nat. Mater.* **2005**, *4*, 864–868.
(36) Shaheen, S. E.; Brabec, C. J.; Sariciftci, N. S. *Appl. Phys. Lett.* **2001**, *78*, 841–843.
(37) (a) Yang, F.; Shtein, M.; Forrest, S. R. *J. Appl. Phys.* **2005**, *98*, 014906/1−10.(b) Hoppe, H.; Sariciftci, N. S. *J. Mater. Chem.* **2006**, *16*, 45–61.
(38) Woo, C. H.; Thompson, B. C.; Kim, B. J.; Toney, M. F.; Frechet, J. M. J. *J. Am. Chem. Soc.* **2008**, *130*, 16324–16329.
(39) Dennler, G.; Scharber, M. C.; Brabec, C. *J. Adv. Mater.* **2009**, *21*, 1323–1338.